Available online at www.worldscientificnews.com

World Scientific News

An International Scientific Journal

WSN 195 (2024) 91-105 EISSN 2392-2192

Optical limiting behaviour and Morphology of Zinc sulfide doped with Methyl green thin film

[1]Alyaa jabar Jerry, [2]Asaad Sayah Hassan, [3,*]Hussain Ali Badran, [3]Riath Chassib Abo-Alhail

[1]Ministry of Education, Directorate of Education, Al-Basma Preparatory School for Girls, Basrah, Iraq

[2]Ministry of Education, Directorate of Education, Nafer Preparatory School for boys, Al-Qadisiyah, Iraq [3]Department of Physics, College of Education for pure sciences, Basrah University, Basrah, Iraq.

[*]Corresponding Email: hussain_badran@yahoo.com

ABSTRACT

We wanted to investigate the optical properties of a zinc sulpfide (ZnS) film that had methyl green (MLG) added to it. This film was made by casting ZnS:MLG onto a micro-glass. After examining the absorption data, we discovered an indirect transition in the fundamental energy band gap (E_{gap}). The optical parameters we looked at were absorbance (A), extinction coefficient (k_{ex}), the real $_{re}$ and imaginary $_{im}$ parts of dielectric constants. Wemple–DiDomenico model was used to determine the dispersion energy and third-order optical nonlinear susceptibility $_{th}^{3}$. A study is being done to determine the ZnS:MLG can be used as an optical limiter.

***Keywords*:** ZnS, ethylgreen, energy gap, optical constant, Optical limiter

(Received 26 June 2024; Accepted 15 July 2024; Date of Publication 19 July 2024)

1. INTRODUCTION

Particularly in recent years, thin, micro, nano films, such as zinc sulpfide (ZnS) that has been doped with organics, dyes, polymer or other ions, have garnered a lot of interest for their potential application in nanotechnology, solar cell and communications device [1]. It is becoming more important to consider optical properties, such as refractive indices (n_r) for a certain wavelength range ranging from ultraviolet to near infrared, as well as E_{gap} values, when determining the appropriate applications for films that have been manufactured [2]. The n_r of optical materials are extremely important for many applications, includes those used in switches and other integrated photonic devices [3]. ZnS is a semiconductor that exhibits a straight transition and possesses a wide gap. Consequently, it could be an essential antireflection layer or coating for hetero-junction solar cells. so that they can function properly [4]. When it comes to detecting, producing, and modifying visible and near-ultraviolet light, this material is an essential component of the device [5]. In particular, ZnS is among the most attractive materials for use in thin film electroluminescent displays and laser diodes that generate blue light [6]. For use in integrated optical devices, such as switches, the refractive indices of optical materials are extremely important variables to consider. One of the most important optical characteristics is the refractive index, which is utilized by prisms, windows, and optical fibers. The portion of the absorption spectrum that is lower in energy provides information about the vibrations of atoms, whereas the portion of the spectrum that is higher in energy contains information about the electronic states of an atom [7,8]. Materials that are thin and have minute defects provide a contribution to light scattering and the associated impairment of the optical response [9]. These imperfections have an impact on the surface's smoothness and the coating's uniformity. Most of the time, the advantage of these materials, which are n-type semiconductors, is that they are more electrically and chemically resilient than other semiconductors. Various methods such as Langmuir- Blodgett (LB), evaporation technique, sputtering, and chemical bath deposition can accomplish the deposition of ZnS thin films. This investigation analyzed the optical characteristics of ZnS: MLG films and made using the cast technique on glass substrates at room temperature. Surface morphology, azimuthal angle Chi, E_d, E_0 and third order optical nonlinear susceptibility $\chi_{th}^{(3)}$, on a spectrum ranging from 300 to 800 nm has been examined at a layer thickness of 5 μm.

II. EXPERIMENTAL SETUP:

In the beginning, we started by dissolving 1 M (0.487 g) of ZnS in HNO_3 and then stirring it for a period of 35 minutes at room temperature. After dissolving 0.4 M (0.304 g) of ethyl green (the chemical composition is shown in the Fig.1) in dimethyl formamide (DMF) and stirring the mixture vigorously at room temperature for half an hour, we proceeded to add the dopant in a proportion of thirty percent to the ZnS.

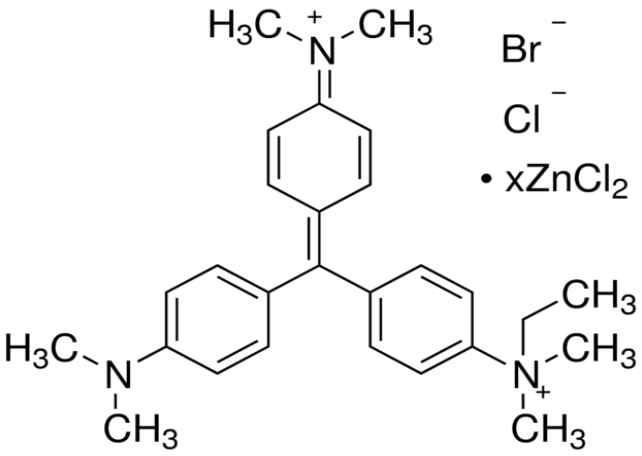

Figure 1. MLG chemical structure.

Using the cast approach, we deposited the stirred solution on the substrate in a horizontal direction in order to create a thickness that was homogeneous throughout. Following a period of two days, we brought the sample from room temperature to a temperature of 80 degrees Celsius, and then we brought it back down to room temperature. We painstakingly clean the substrate before film deposition by first immersing it in a 10% $K_2Cr_2O_7$+H_2SO_4 cleaning solution for an hour in an ultrasonic path, and then washing it with distilled water and an organic solvent (acetone). This process is repeated until the substrate is completely clean. In conclusion, prior to making use of the substrate, we dried it.

3. SURFACE ANALYSIS:

One of the most important aspects of optical devices is the surface topography characterization. When it comes to diffusion transmission, average roughness tends to be more favourable. Roughness characteristics are utilised

in linear and nonlinear optics for a variety of purposes, including electrooptical effects [10], sensitive optical fibres [11], and optical data storage[12]. An atomic force microscope was utilised in order to investigate the ZnS:MLG film. The use of image processing can be investigation of the surface morphology of film. For the purpose of imitating an optical method of assessing surface roughness, it is utilised. Figure 2 depicts a surface

scan of a thin film that was seen using a two-dimensional microscopic imaging technique. When examined more closely, each picture displays two distinct morphological traits, which are denoted by the letters a and b. The first thing to note is that several scales of granular characteristics are present in the film, and these qualities are virtually evenly distributed in some areas. Within the sample, there was no discernible categorization. Fig.2 shows the angle between the incident beam and the scattering plane, in degrees vs. film intensity with azimuthal angle Chi, ranging from 0 to 360, displayed in Figure 2b to illustrate the relationship between the two variables.

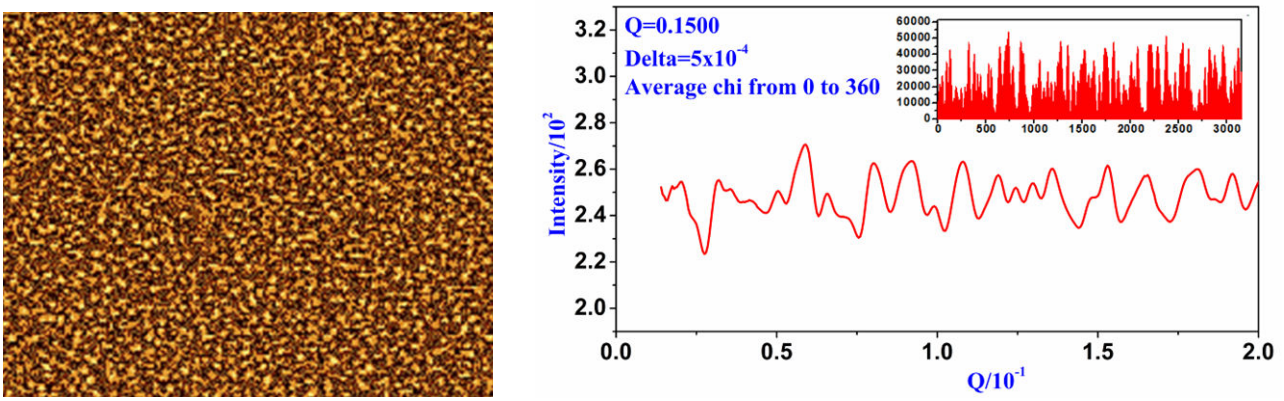

Figure 2. (a). Atomic force microscope of ZnS doped with MLG film. (b) Azimuthal angle Chi of film.

4. RESULT AND DISCUSSION:

Quantification of A and T in the wavelength (λ) range of 300-700nm was accomplished by the use of UV-visible spectroscopy type CE 3055. Figure 3 illustrates the link that exists between the absorbance (A) of the film and the wavelength on the spectrum. As can be seen in the image, the transition from $\pi \rightarrow \pi^*$ that is represented by the peak in the curve, which occurred at a λ of 500nm.

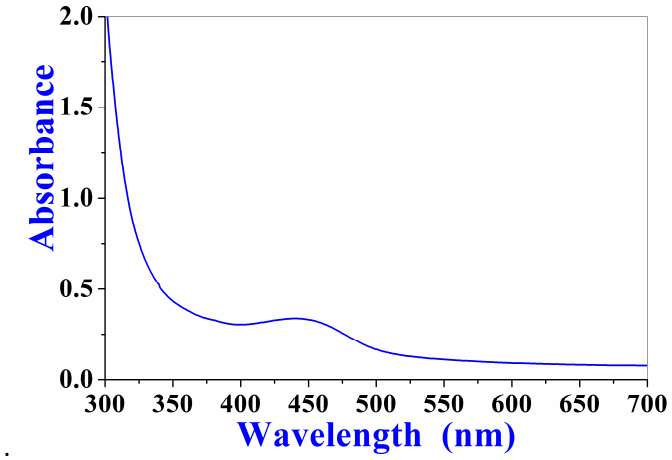

Figure 3. Spectral absorption vis wavelength of ZnS:MLG film.

Increasing the wavelength from 300 to 425 nanometers resulted in a rise in the transmittance percentage, which went from forty percent to fifty-five percent in the ultraviolet-visible zone. The image makes it abundantly evident that there is a decrease in the amount of light that is transmitted from the film in the λ range of 425 to 550 nm. This indicates that part of the light was absorbed by ZnS:MLG. Transparency was achieved by the polymer at longer wavelengths (greater than 550 nm), and there was neither scattering nor absorption of light ($R+T=1$). ZnS:MLG film was reported to exhibit a behaviour that was comparable to that described in [13]. While the T spectra in the UV-Visible area revealed that the T percent grew from 40% to 55%, the T spectra in the UV-Visible region showed that the λ increased from 300 to 425 nm increased. The figure indicates a decrease in light transmission from the film between 425 and 550 nm, suggesting that ZnS:MLG absorbed some of the light. At longer wavelengths (>550 nm), the film become transparent, absorbing or scattering light in the process (R+T = 1). The thin film of ZnS:MLG showed the same pattern of behaviour [14].

As the frequency changes, Figure 4 shows how the film's reflectivity changes. The figure shows that the R% drops sharply as the λ goes from (300–425 nm) to (500–700 nm), with 500 nm being the wavelength with the most reflection.

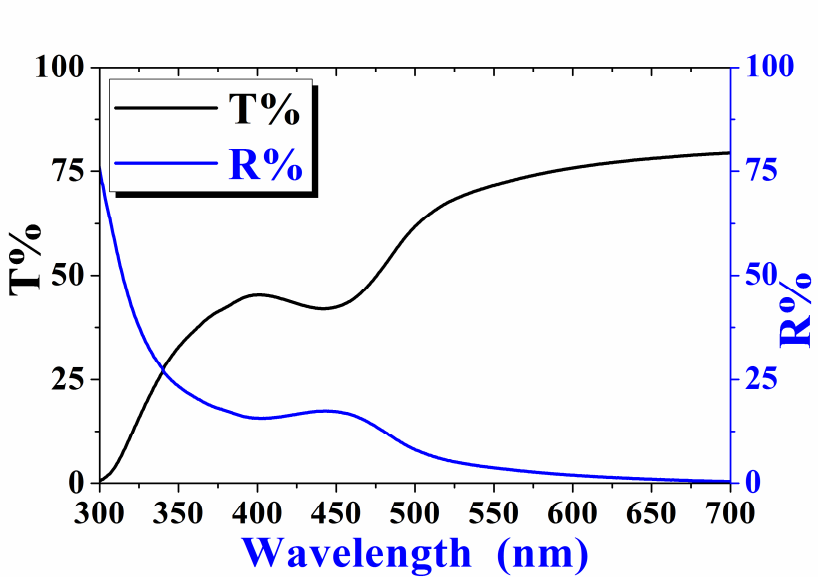

Figure 4. Behavior of both T and R of the ZnS:MLG film.

Beer Lamberts' formula (=2.303 A_{ab}/T_{th} [15-18]), where A_{ab} is the optical absorbance andis the film T_{th} thickness, can be used to compute the absorption coefficient (α_{op}) from observed absorbance data [19]. Figure 5 shows the relationship between α_{op} and hv for the prepared ZnS:MLG film. As shown in the figure5 , the photon energy is clear at 1.75eV to 3.5eV, with a broad peak at 2.8eV, then there is a smooth rise in the curve and no peaks are formed again through 2.8eV and up to 3.25eV, before the curve rises only at high energies.

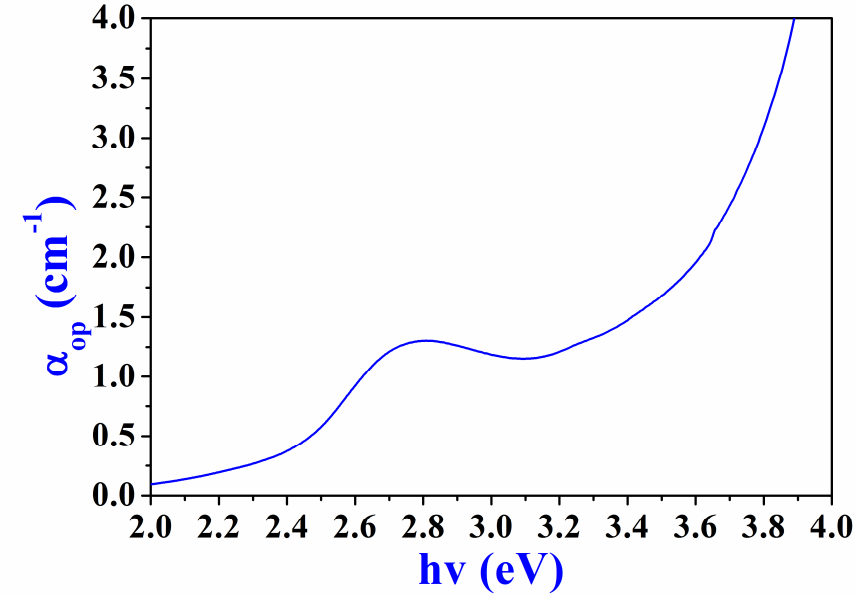

Figure 5. α_{op} agenest hv.

The mathematical relationship known as extinction energyfrom the relation finedcan be k_{ex} ($k_{ex} = \alpha_{op}\lambda/4\pi$ [20,21]). The refractive index n can be determined from R, of the Zn:GML film and their k_{ex} by the relation [22,23]:

$$n = \frac{1+R}{1-R} + \sqrt{\frac{4R}{(1-R)^2} - k_{ex}{}^2} \quad (1)$$

A representation of the relationship between wavelength , n and k_{ex} is shown in Figure 6. There is a strong indication from the statistics that the values of the n and k_{ex} drop as the λ increases in the range spanning from 300 to 400 nanometers. These values dropped as the wavelength grew in the range (510–800nm), which is where the peak occurs. The peak occurs about 470nm.

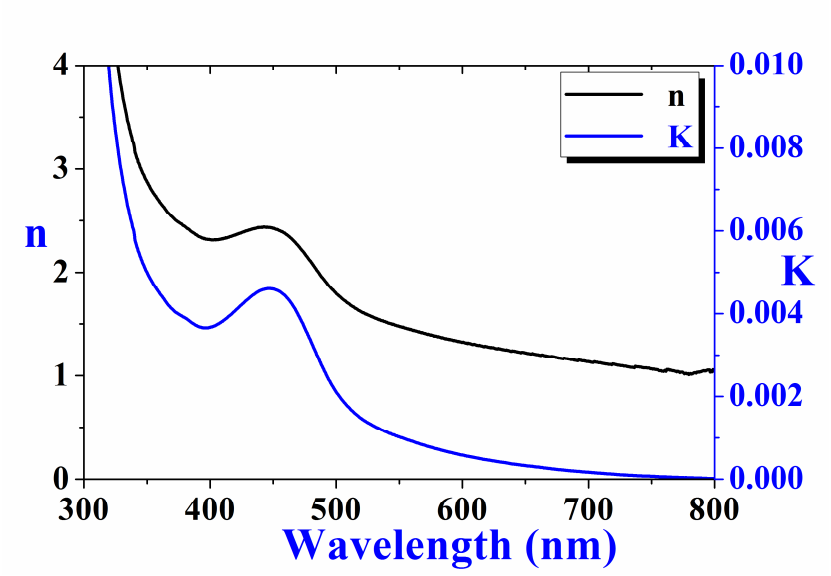

Figure 6. The relationship between n, k_{ex} and wavelength.

There is a correlation between the energy of the photon and α_{op} at the region of both crystalline and amorphous semiconductors' basic absorption edge. A more generic version of the absorption coefficient was taken into consideration for direct transitions, and it was expressed as a function of the hv [24,25]:

$$\alpha_{op} hv = a(\alpha_{op} hv - E_{gap})^{\tilde{m}} \quad (2)$$

$$\alpha_{op} hv = b(\alpha_{op} hv - E_{gap})^{\tilde{m}} \quad (3)$$

where v is the frequency of the incident photon, $\tilde{m}$ is the number which characterizes the optical processes. $\tilde{m}$ has the value 1/2 for the direct allowed transition, 3/2 for a forbidden direct allowed transition and 2 for the indirect allowed transition, a and b are constants. When the straight portion of the graph of $(\alpha_{op} hv)^{\tilde{m}}$ against hv is extrapolated to α_{op} =0 the intercept gives the transition band gap [26]. Fig.7 shows the plot of $(\alpha_{op} hv)^{0.5}$ against photon energy for indirect transition. This curve was used to calculate the fundamental energy gap, which was found to have a value of 2.17eV and photon energy of 1.72eV.

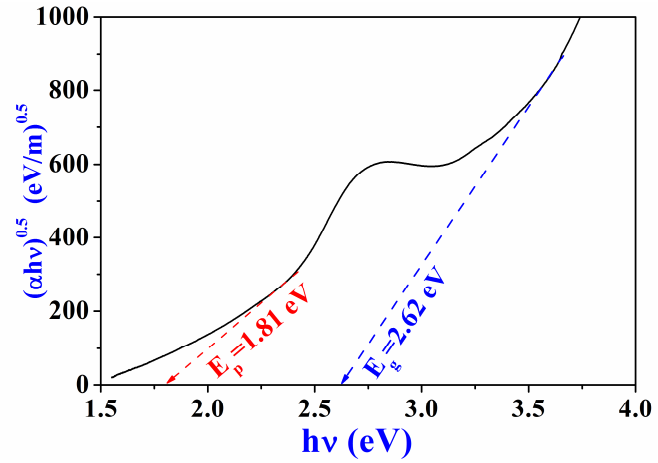

Figure 7. The relation between $(\alpha_{op} h\nu)^{0.5}$ against photon energy

ε_r and ε_i can be calculated by using equations [27,28]:

$$\varepsilon_r = n^2 - k_{ex}^2 \tag{4}$$

$$\varepsilon_i = 2nk_{ex} \tag{5}$$

Figure 8 illustrates the relationship between ε_r and ε_i. Although ε_r and ε_i parts seem to follow the same trend, the ε_r part's values are higher than the ε_i part's. The relationship between the ε_r and ε_i and $h\nu$ indicates that there are interactions between photons and electrons in the film at this energy range. The shapes of ε_r and ε_i parts reflect these interactions. They cause peaks to form in the dielectric spectra, depending on the type of the material. For instance, the ZnS:MLG film showed a high peak around 2.55eV. The high photon's energy exceeded 3.5eV sharply increased ε_r and ε_i parts of the dielectric constant.

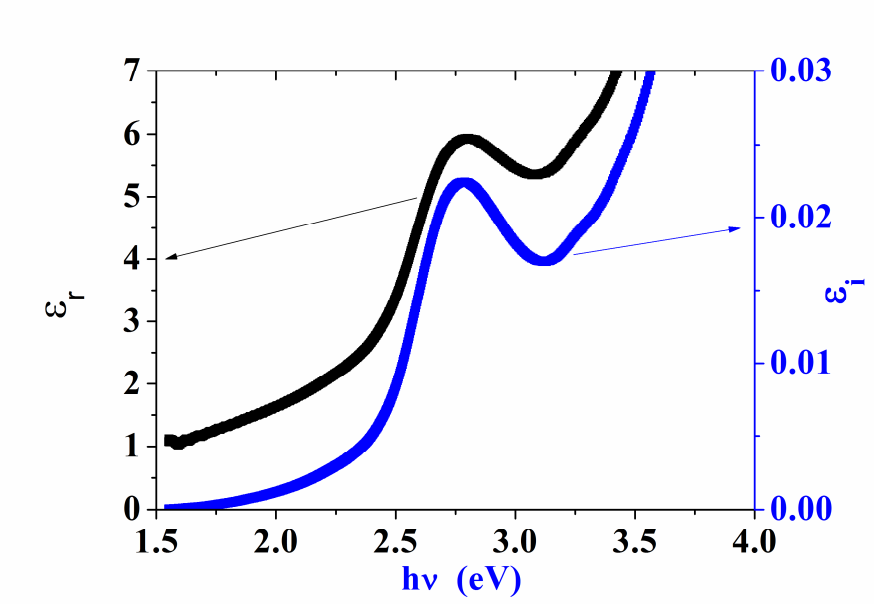

Figure 8. ε_r and ε_i against $h\nu$

5. DESPERATION PARAMETER:

The moments of the optical spectra can be calculated by using equations below [29,30]:

$$E_0^2 = \frac{\ddot{M}_{-1}}{\tilde{M}_{-3}} \quad \text{and} \quad E_d^2 = \frac{\ddot{M}_{-1}^3}{\tilde{M}_{-3}} \tag{6}$$

Both the $\ddot{M}_{-1}$ and $\tilde{M}_{-3}$ moments were determined by using the equations presented above, and the results are presented in table 1. At a high frequency, the characteristics of the ZnS:MLG film that was tested might be considered as a single oscillator with λ_0 during the investigation. By using the following straight-forward classical dispersion relation, one is able to get the high frequency of the dielectric constant [30]:

$$\frac{n_0^2 - 1}{n^2 - 1} = 1 - [\frac{\lambda_0}{\lambda}]^2 \tag{7}$$

where λ_0 indicated the average interband oscillator wavelength, and λ is the incident photon wavelength. Most resercher say that the Miller rule works well for clear and nonlinear infrared frequencies [31,32]. It equalises the third-order susceptibility, χ_{th}^3, and linear susceptibility χ_{lin}^1 using the relation [33-38]:

$$\chi_{th}^3 = A(\chi_{lin}^1)^4 = A\left(\frac{E_0 E_d}{4\pi(E_0^2 - (h\nu)^2}\right)^4 = \frac{A(n^2-1)^4}{(4\pi)^4} \tag{8}$$

Where A is the constant. We calculated the third-order nonlinear susceptibility , χ_{th}^{3} of ZnS:MLG film using equation 8. The estimated value of χ_{th}^{3} is equal to 8. 17×10^{-12} esu for n_0=2.6.

Table 1: The linear third-order nonlinear parameters for ZnS:MLG film.

E_g (eV)	2.17	E_{phonon} (eV)	1.72	M $_{-1}$	10.3
M $_{-3}$ $(eV)^2$	1.56	λ_0 (nm)	664	S_0 $(m)^{-2}$	1.33×10^{13}
E_u (meV)	168	N/m*(m^{-3}Kg)	9.8×10^{60}	F	30
E_0 (eV)	2.57	E_d (eV)	11.68	χ_{th}^{3} (esu)	8.17×10^{-12}
$\varepsilon_\infty(2)=n_0^2$	6.88	$\varepsilon_\infty(1)=n^2$	5.58	n_0	2.6

6. OPTICAL LIMITING:

When the prevalent intensities are at their peak, optical limiters are devices that reduce the intensity of optical beams while still allowing light to pass through at low levels [39]. A perfect optical limiter is completely transparent up to a certain intensity level, and once it reaches that level, the transmitted intensity is capped at a fixed amount. This is the case even when the intensity is low. Irradiation of high intensity can be protected from the human eye and sensitive optical sensors by using these materials, which are beneficial for this purpose [40]. It is possible to accomplish optical limiting (OLMG) in the presence of an aperture by varying the power that the laser receives as input and monitoring the power that the sample receives as output [41]. Figure 9 illustrates the OLMG findings of the ZnS:MLG film. The sample demonstrates an OLMG effect. There is a linear relationship between the output of an optical limiter and the incident laser beam intensity when the incident intensity is low, according to Beer's law. The output intensity of the sample, on the other hand, deviates from linearity when the incidence intensity is large. Additionally, a nonlinear link between the output and the incident intensity is seen, which is referred to as the limiting threshold (LMTH). The intensity of the output reaches a plateau, and it reaches its maximum level when the incident intensities continue to increase. Figure 10 illustrates how the intensity of the light that is transmitted changes as a function of the intensity of the light that is initially incident. In general, the OLG ability of a sample is evaluated by employing a LMTH, which is defined as the incoming input intensity or power that, when it is below that threshold, results in a 50% reduction in transmission 7.18 milliwatts was determined to bethe value of the sample's OLG thresholds.

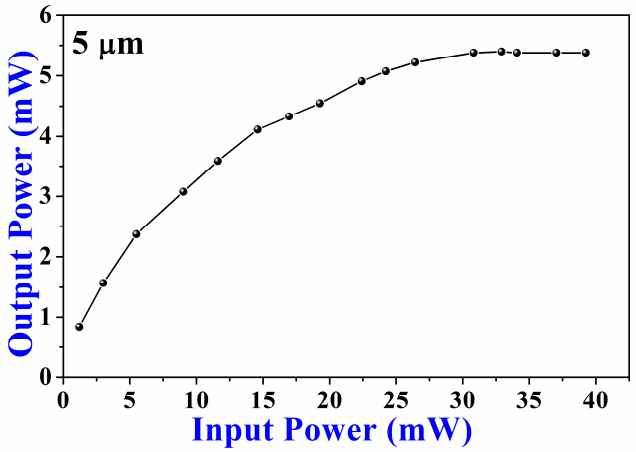

Figure 9. limiting power of ZnS:MLG film.

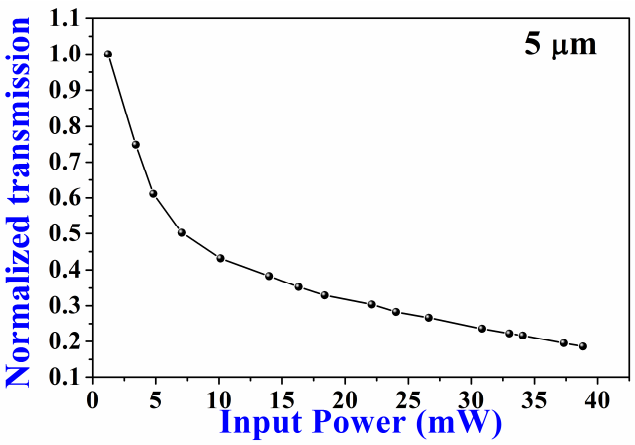

Figure 10. Threshold power for ZnS:MLG film.

CONCLUSIONS:

In the current investigation, we determined the optical constants by calculating the optical properties of a ZnS:MLG film that was formed by employing the casting technique on a substrate at Rm and calculating the optical characteristics. During the examination, the surface morphology, E_d, E_0, S_0 and the optical moments M_{-1}, M_{-3} and χ^3_{th} were all taken into consideration. Optical absorption was caused by an indirect transition, which had an energy gap of 2.17eV and phonon energy of 1.72eV. This sort of optical transition was responsible for the phenomenon. We conducted an investigation into the OLMG characteristics of Zns:MLG film, and the findings showed that the film displayed this effect.

References

[1] R. K.F Alfahed, Ahmed S. Al‑Asadi, Hussain Ali Badran, Khalid I. Ajeel, Structural, morphological, and Z-scan technique for a temperature controllable chemical reaction synthesis of zinc sulfide nanoparticles. *Applied Physics B* 125 (2019) 48, https://doi.org/10.1007/s00340-019-7154-7

[2] A. Henglein.Small-particle research: physicochemical properties of extremely small colloidal metal and semiconductor particles. *Chem. Rev.* 89(1989) 1861. https://doi.org/10.1021/cr00098a010

[3] F.A. Al-Saymari, H.A. Badran, A.Y. Al-Ahmad, C.A. Emshary, Time dependent diffraction ring patterns in bromothymol blue dye doped PMMA film under irradiation with continuous wave green laser light. *Indian J. Phys.* 87(2013) 1153–1156. https://doi.org/ 10.1007/s12648-013-0334-0.

[4] Burak K., R.K. Fakher Alfahed, Ahmed S. A., Hussain A. B., Morphological, structural, optical, and photovoltaic cell of copolymer P3HT: ICBA and P3HT:PCBM, *Optik* 204 (2020) 164153. https://doi.org/10.1016/j.ijleo.2019.164153

[5] Fadhil A. Tuma, Mohammed T. Obeed, Alyaa A. Jari, Hussain Ali Badran, T.A. Alaridhee, Effect of gamma ray on self-induced diffraction patterns of organic compound Poly (methyl-methacrylate films), *Results in Physics* 52 (2023) 106858. https://doi.org/10.1016/j.rinp.2023.106858

[6] H.G. Lazim, K.I. Ajeel, H.A. Badran, The photovoltaic efficiency of the fabrication of copolymer P3HT: PCBM on different thickness nano-anatase titania as solar cell. *Spectrochim. Acta Part A Mol. Biomol.* Spectrosc. 145 (2015) 598–603. https://doi.org/10.1016/j.saa.2015.02.096

[7] Sharma T P, Patidar D, Saxena N S and Sharma K. Measurement of structural and optical band gaps of Cd1-xZnxS (x = 4 and 6) nanomaterials. *Indian J. Pure and Appl. Phys.* 44 (2006) 125-128.

[8] L. Cai, C. Wang. Carbon Nanotube Flexible and Stretchable Electronics. *Nanoscale Res. Lett*. 10(10) (2015) 320. https://doi.org/10.1186%2Fs11671-015-1013-1

[9] R. K. Fakher Al-Fahed, Alaa A. Rashad, Munaf S. Majeed, and Hussain A. Badran, Chemical Polymerization Method to Synthesize Polyaniline as a Novel Anode Catalyst in Microbial Fuel Cell, *Polymer Science, Series B*, 63(6) (2021) 773-780. https://doi.org/10.1134/S1560090421060026

[10] R.K.F. Alfahed, H. A. Badran, A.T.Yousif, A.S. Noor, Investigation of third order nonlinearity of Ethidium bromide doped deoxyribonucleic acid (DNA). J Phys Conf Series 1963 (2021) 012136. https://doi.org/10.1088/1742-6596/1963/1/012136

[11] Tuma F.A., H.A.Badran, A.H. Harith, R. Ch. Abul-Hail, Azimuthal Angle Scan Distribution, Third Order Response, and Optical Limiting Threshold of the Bismarck Brown Y:PMMA Film, *Current optics and photonics*,7(6) (2023) 731-721

[12] H. A. Badran, N. A. Hussein Al-Assady, H. A. Hasan, R. Ch. Abul-Hail, R. K. Al-Fahed, Synthesis, DSC Properties, Surface Morphology and the Third-Order Behavior Studies of a Conducting Polymer. *Polymer Science, Series B,* 65(6) (2023) 858–872. https://doi.org/10.1134/S1560090423600237

[13]W.Wang, Z.Liu, C. Zheng, C. Xu. Y. Liu, G. Wang. Synthesis of CdS nanoparticles by a novel and simple one-step, solid-state reaction in the presence of a nonionic surfactant. *Materials Letters* 57 (2003) 2755-2760. https://doi.org/10.1016/S0167-577X(02)01371-X

[14] H.A. Badran, K. I. Ajeel, H.G. Lazim, Effect of nano particle sizes on the third-order optical non linearities and nanostructure of copolymer P3HT: PCBM thin film for organic photovoltaics. *Mater Res Bull* 76 (2016) 422–430. http://dx.doi.org/10.1016/j.materresbull.2016.01.005

[15]Al-Salihi A, Salim RD, Alfahed RKF, Badran HA. Effect of Solar radiation induced and alpha particles on Nonlinear behavior of PM-355 film. *IOP Conf. Series. Mater Sci Eng*, 928 (2020) 072056. https://doi.org/10.1088/1757-899X/928/7/072056.

[16] H. A.Badran, A.A. Hanan, A. R.K.F, I.A. Khalid. Second-order hyperpolarizability and nonlinear optical properties of novel organic compound-doped poly (O-methoxyaniline) polymer film. *J Mater Sci Mater Electron* 32 (2021) 14623–41. https://doi.org/10.1007/s10854-021-06021-2.

[17] A.T. Fadhil, H. A.Badran, H.A.Hussan, R. Ch.Abul-Hail, Effect of 1,4-dihydroxyanthraquinone dye on The dispersion parameters of poly(methyl methacrylate) polymer composites, *World Scientific News* 184 (2023) 25-37

[18] A.Y. AL-Ahmad, M.F. AL-Mudhaffer, H.A. Badran, C.A. Emshary, Nonlinear optical and thermal properties of BCP:PMMA films determined by thermal self-diffraction. *Opt. Laser Technol.* 54, (2013) 72–78. https://doi.org/10.1016/j.optlastec.2013.05.009

[19] H.A. Badran, A.A. Al-Fregi, R.F. Alfahed, A.S..Al-Asadi, Study of thermal lens technique and third-order nonlinear susceptibility of PMMA base containing 5′, 5′′- dibromo-o-cresolsulfophthalein. *J Mater Sci Mater Electron*, 28 (2017)17288–7296. https://doi. org/10.1007/s10854-017-7661-4

[20] J.Pantoja Enriquez, Effect of annealing time and temperature on structural, optical and electrical properties of CdS films deposited by Cbd, *Chalcogenide Lett*. 10 (2013) 45–53.

[21] Mark Fox, Optical Properties of Solid, 2nd ed., Oxford University Press, Inc., New York, 2001.

[22] J. Gang Gao, J. Xu, B. Chen, Q. Jin Zhang, A quantitative structure-property relationship study for refractive indices of conjugated polymers, *J. Mol. Model.* 13 (2007) 573–578

[23] H. A. Hasan, N. A. Hussein Al-Assady, H. A. Badran , R. K. Alfahed , K. I. Ajeel, The influence of temperature on structural and third order nonlinear properties of cadmium sulfide nanoparticle films prepared by chemical reaction method, *Materials Research Bulletin* 170 (2024) 112554. https://doi.org/10.1016/j.materresbull.2023.112554

[24] T. P Sharma, D. Patidar, N. S. Saxena, K. Sharma, *Indian J. Pure and Appl. Phys.* 44 (2006) 125.

[25] H. A. Badran, A.Y. Taha, A. F. Abdulkader, C. A. Emshary Preparation and study of the electrical and optical properties of a new azo dye (4-Acetaminophenol-[2- (4-Azo)]-4- amino dipheyl sulfone). *Journal of Ovonic Research* 8 (2012)161–170.

[26] R.F. Alfahed, A.S. Al-Asadi, H. A. Badran, K.I.Ajeel. Structural, morphological, and Z-scan technique for a temperature-controllable chemical reaction synthesis of zinc sulfide nanoparticles. *Appl Phys B*,125(2019) 48. https://doi.org/10.1007/s00340-019-7154-7

[27] H. A. Badran. Study on Optical Constants and Refractive Index Dispersion of Neutral red Doped Polymer Film. *Am J Appl Sci,* 9 (2012) 250-253. https://doi.org/10.3844/ajassp.2012.250.253

[28] A. A. Hussain, A. A. Musa, R. K. F. Alfahed, H. A. Badran. Diffracting samples, Nonlinear optical properties and morphology for (2- hydroxyphenyl) [2-(2-methoxybenzylideneamino)- 5-methyl phenyl] telluride film. *AIP Conf Proc* 2290 (2020) 050049. https://doi.org/10.1063/5.0027845

[29] H. A. Al-Hazam, R. K. F. Alfahed, I.Abdulameer, H. A. Badran, S. S. Hussain, A. Alsalihi, K. I.Ajeel Preparation and optoelectronic studies of the organic compound [2-(2,3-dimethyl phenylamino)- *N*-Phenyl benzamide doped (PMMA)]. *J Mater Sci Mater Electron* 30 (2019)10284-10292. https://doi.org/10.1007/s10854-019-01365-2

[30] H. A. Hasan, A.H.A. Nadia, H. A. Badran, R. K. Alfahed, K. I.Ajeel, Effects of temperature on structural and linear/nonlinear optical properties of CdS nanoparticles film deposited by chemical reaction method. *Opt Quant Electron* 55 (2023) 555. https://doi.org/10.1007/s11082-023-04835-4

[31] H.A.Badran, A.Al-Maliki,R.K.F.Alfahed, S.B.Ali, A.Y.Al-Ahmad, F.A. Al-Saymari, S.E.Rita Synthesis, surface profile, nonlinear reflective index and photophysical properties of curcumin Compound. *J Mater Sci: Mater Electron* 29 (2018)10890-10903. https://doi.org/10.1007/s10854-018-9167-0

[32] H.S. Shaaker, A. Hussain, H. A. Badran, Determination of the optical constants and optical Limiting of doped malachite green thin films by the spray method. *Adv Appl Sci Res* 3(2012)2940–2946

[33] S.H. Wemple, M. DiDomenico, Behavior of the electronic dielectric constant in covalent and ionic. Materials, *Phys Rev B* 3 (1971)1338–1351. https://doi.org/10.1103/PhysRevB.3.1338

[34] I. Abdulameer, J. B. Sattar, A. Abdalrahman, H.A.Badran, Gamma irradiation impact on the morphology and thermal blooming of sodalime glass. *AIP Conf Proc* 2290 (2020) 050038. https://doi.org/10.1063/5.00314 73

[35] H. A. Badran, T.Y.A. Abu, R.K.F. Alfahed, Study the Effect of Concentration on the Evolution of Far Field Diffraction Patterns of Bromocresol Purple and Congo Red Solution. *J Phys Conf Series*,1963 (2021) 012013. https://doi.org/10.1088/1742- 6596/1963/1/012013

[36] V. Narayanan, R.K. Thareja, Harmonic generation in ZnO nanocrystalline laser deposited thin Films. *Opt Commun* 260 (2006)170. https://doi.org/10.1016/j.optcom.2005.09.073

[37] R.K.F. Alfahed, A. Imran, M.S. Majeed, H. A.Badran, Photoluminescence characterizations and nonlinear optical of PM-355 nuclear track detector film by alpha-particle and laser irradiation. *Physica Scripta* 95(2020) 075709 (8pp). https://doi.org/10.1088/1402-4896/ab7e33

[38] H. A.Badran, R. Ch. Abul-Hail, T.O. Mohammed Study on effect of Gamma radiation on some linear and nonlinear properties of Pyronine Y. ,*AIP Conf Proc* 2290(2020) 050035. https://doi.org/10.1063/5.0027452

[39] K. A. AL-Adel, H. A. Badran, χ^3 measurements and optical limiting in Bismarck Brown Y dye, *Inter. J. of Emerging Technologies in Computational and Applied Sciences (IJETCAS)*,8 (2014) 64-68

[40] R. K.F. Alfahed, I. Abdulameer, H. A. Badran, A. Al‑Salihi, Synthesis, optical limiting behavior, thermal blooming and nonlinear studies of dye‑doped polymer films, *J. of Materials Science: Materials in Electronics* 31 (2020)13862–13873, https://doi.org/10.1007/s10854-020-03946-y

[41] H. A. Badran , K. A. AL-Adel, Optical Nonlinear Properties and Optical Limiting Effect of Congo red dye under CW Laser, *Misan Journal for Academic Studies*, 11(21) (2012) 1-9.